Journal of Sciences, Islamic Republic of Iran 30(3): 241 - 250 (2019) http://jsciences.ut.ac.ir
University of Tehran, ISSN 1016-1104

Role of Hydrogen Transfer and Ionic Bonding on RR, SS and RS Medetomidine Conglomerates/Acids Stability: A Theoretical Study

V. Zarei[*1], N. Javadi[2], Z. Ghahramani[3], H. Fakhraian[2]

[1] *Department of Chemistry, Faculty of Science, University of Shiraz, Shiraz, Islamic Repoblic of Iran*
[2] *Department of Chemistry, Faculty of Science, University of Imam Hossein, Tehran, Islamic Repoblic of Iran*
[3] *Department of Chemistry, Firouzabad Branch, Islamic Azad University, Islamic Repoblic of Iran*

Received: 13 June 2018 / Revised: 9 October 2018 / Accepted: 15 December 2018

Abstract

This study focuses on RR, SS and RS medetomidine (MM) and inclusion of several achiral acids to distinguish which acid can help conglomerate formation instead of crystallizating racemic mixtures by defining the low-lying energy of their structures. Favorable orientation of acids was determined in interaction with the MM enantiomers after optimization. The most noticeable interactions include hydrogen transfer from acids to nitrogen (N) atom of the MM enantiomers, which was confirmed through quantum theory of atom in molecule (QTAIM) and natural bond orbital (NBO) analysis. In addition, nature and source of change of these bonds were investigated by determination of significant donor-acceptor interactions. The results revealed for obtaining RR and SS conglomerates; oxalic acid solvent provides the optimum stability. Furthermore, application of propanoic acid solvent should be neglected since MM crystallization is nonspontaneous with this solvent. Therefore, oxalic acid is the acid of choice for preferential conglomerate formation.

Keywords: Quantum chemistry; Conglomerates; Hydrogen transfer; Medetomidine; Stability.

Introduction

Chirality is one of the most essential issues in biological systems and specifically in the pharmaceutical industry [1]. Different research groups have stated that chirality can provide different properties and has effects on the behavior of chiral compounds in interaction with other compounds, e.g. [2, 3]. Furthermore, the chirality issue can get more complicated since many chiral drugs are delivered to body as racemic mixtures [4-6]. Racemic mixtures contain two enantiomers which have identical physiochemical properties except for the sign of optical rotation. If achiral reaction medium be used, then a racemate, that is a mixture composed of equal amounts of the two enantiomers, will form. As a consequence, the enantiomeric mixture should be separated into the pure enantiomers for pharmaceutical purposes [7]. So that chirality can leads to diverse pharmacological impacts and activities, drug side effects, conglomerate behavior and optical activity [2, 8-10]. Therefore, scientists believe that concerning about chirality is an integral part of drug design and development.

[*] Corresponding author: Tel: +989176309527; Fax: +987132292889; Email: vahidzarei181@gmail.com

One of the interesting chiral compounds that demands separation is 4-[1-(2,3- Dimethyl-phenyl)ethyl]-3H-imidazole (medetomidine (MM)). MM is a highly selective agonist of alpha-2 adrenergic that is usually used as a sedative, pain relief and anti-stress drug. It has one chiral center located on the Carbon atom that links the two phenyl and imidazole rings [11-14] and supplied in a the form of racemic mixture of its two optical enantiomers, i.e. dexmedetomidine (S enantiomer) and levomedetomidine (R enantiomer). Dexmedetomidine is the active medicine, which has a selectivity ratio of 1620/1 (α2/α1) that is 5–10 times higher than that for detomidine (260/1) and xylazine (160/1) drugs. For small animals, MM is superior to xylazine due to low affinity for α-1 adrenoceptors and interacting with central imidazoline receptors. Also, it can develop an anti-arrhythmic property mediated by an imidazoline/vagaltone stimulation [11-14]. Moreover, MM-hydrochloride salt is commonly used as a sedative, analgesic, and anesthetic premedication in animals [15] while Dex-MM is used in human anesthesiology as an active part [16].

Similar to any other chiral compound, MM crystalizes as racemate and therefore it may be of three different types. First, conglomerate: they are result of spontaneous resolution of enantiomers into separate crystals. It means that the two enantiomers crystallize separately and homochirally and one pure S enantiomer block and one pure R block forms aside each other. Second, it is also the most common type, the racemic crystal. Final, formation of a solid solution that contains R and S mixture with unequal amounts and disordered arrangement were studied [1, 10]. So, RR, SS and RS forms of MM exist as conglomerate and racemate mixtures with unique properties [16].

Employing of the MM enantiomers as a pharmaceutical compound, MM separation as a conglomerate is mandatory. One separation option is resolution of the conglomerate by preferential crystallization or 'entrainment' or resolution by enzymes or bacteria that has been performed on some racemates in large scale, e.g. amino acids. Another option is using another chiral compound and resolving the enantiomers through chromatography [7].

The chromatographic method is the chosen approach by pharmaceutical industry. However, this technique is very costly due to requiring another racemic mixture. Therefore, as alternative solution can replace this procedure with a cheaper approach. One alternative strategy is obtaining conglomerate of the enantiomer of interest using an available achiral compound.

In this respect, the current study attempts to investigate theoretically about MM and find out which achiral acid can be used to provide conditions for preferential conglomerate formation rather than racemic mixture crystallization. To date, to the best of our knowledge, only one experimental research has been conducted on MM and the separation of its racemic mixture to form conglomerate by Fakhraei et al [8,15] and no theoretical approach has considered MM conglomeration.

Here, we use Hartree Fock (HF) and density functional theory (DFT) to obtain the structures of R and S enantiomers and the RR, SS and RS forms. Further, we focus on the stability related energies, NBO and AIM analysis to define the best acid for conglomerate crystallization and identify the underlying nature of events and interactions.

Materials and Methods

Computational Methods

Geometry optimizations and calculations of energy and spectra were carried out by using Gaussian 09 program package [17] in the framework of density functional theory (DFT) method and 6-31++g(d,p) basis set [18, 19]. To confirm that the structures refer to the corresponding local minima, vibrational frequencies were calculated and no imaginary frequency was obtained for any of the structures such as other report [20]. Further, the stability of the systems was evaluated through computing energies of binding (E_{bind}), interaction (E_{int})and Gibbs free energy (ΔG) according to equations [1] to [3], respectively.

$$E_{bind} = E_{complex} - (E_{MM} + E_{acid}) \quad [1]$$

$$E_{int} = E_{bind} - (\Delta E_{MM} + \Delta E_{acid}) \quad [2]$$

$$\Delta G = \sum \Delta G_{complex} - \sum(\Delta G_{MM} + \Delta G_{acid}) \quad [3]$$

In these equations, $E_{complex}$, E_{MM} and E_{acid} are the total energy of the complex, MM and the acid. In addition, ΔE_{MM} and ΔE_{acid} are respectively the deformation energies of MM and the acid, respectively, where difference between the energy of the free molecule in the gas phase and the energy of the isolated and distorted molecule in its complex form is called deformation energy. Also, $\Delta G_{complex}$, ΔG_{MM}, and ΔG_{acid} are respectively free energies of the complex, MM and the acid.

Moreover, geometrical information is completed by the results of the quantum theory of atom in molecules (QTAIM) [21] and natural bond orbital (NBO) analysis [22]. In one hand, based on the QTAIM theory, electron density $\rho(r)$ and Laplacian $\nabla^2\rho(r)$, electronic energy density H(r), electronic kinetic energy density G(r) and electronic potential energy density V(r) descriptors are calculated at the bond critical points (BCPs) and ring

critical points (RCPs). On the other hand, type of bonds, depletion of occupancies, percent of Lewis and non-Lewis and stabilization energies [22, 23] are obtained by NBO analysis. The stabilization energy (E^2_{ij}) in equation [4] includes interaction Hamiltonian$\hat{H}$, orbital energies E_j and E_i and also $\langle i \left| \hat{H} \right| j \rangle$ that is the matrix element.

$$E_{ij}^2 = \frac{\left|\langle i|\hat{H}|j\rangle\right|^2}{E_j - E_i} \quad [4]$$

Results and Discussion

Geometries of the compounds

Ground state structures of the organic acids, hydrochloric acid and acetic acid were investigated at B3LYP/6-31++g(d,p) level of theory, which are presented in Figure 1, in order to obtain microscopic insight about the interaction of acids with the enantiomers of medetomidine (MM). These structures were evaluated against experimental reports such as geometry parameters and nuclear magnetic resonance (NMR) and infrared (IR) spectra (for example MM.OX) to approve the selected method/basis set [8, 24] in Table 1 and Figure 2, respectively. The experimental and theoretical chemical shift values regarding MM are listed in Table 1 and validate the employed level of theory to be appropriate for this study. It is noteworthy that other computational levels including B3LYP, MP2 and G3MP2 with different basis sets were also used but their results were not satisfying according to experimental results.

The R-MM and S-MM enantiomers were optimized in the RR, SS and RS states to simulate their structures in their crystallized cells, observe the arrangement of enantiomers, investigate their stability and determine the best acid that can be applied in MM conglomerate crystallization procedure. During the optimization

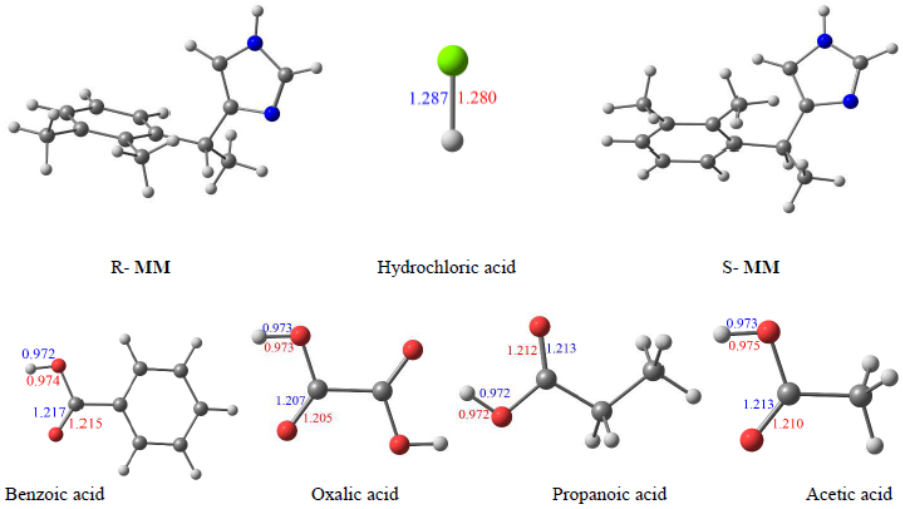

Figure 1. Obtained optimal structures of all acids and (R), (S)-**MM** enantiomers at the selected level of theory. The values written in blue and red are the bond lengths from this study and the experiment values [24], respectively.

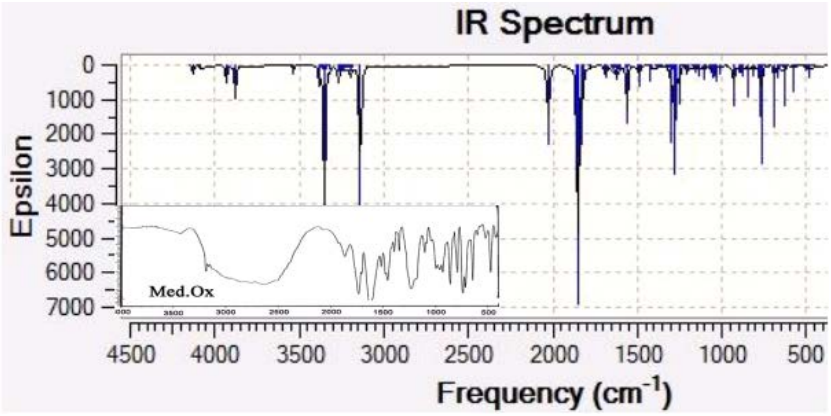

Figure 2. Theoretical and experimental (small spectrum) IR spectra of MM.OX complex [8].

Table 1. Comparison of the experimental [8, 24] and computational NMR spectra data for MM.

Hydrogen type	Experimental data		Computational data	
	Chemical shift	integral	Chemical shift	integral
CH_3 (1)	2.23	3	2.65	3
CH_3(2)	2.15	3	2.35	3
CH_3 (3)	1.25	3	1.63	3
H (4)	4.33	1	4.37	1
H (Aromatic)	6.63-7.25	5	6.27-7.72	5
H (5)	10.26	1	8.30	1

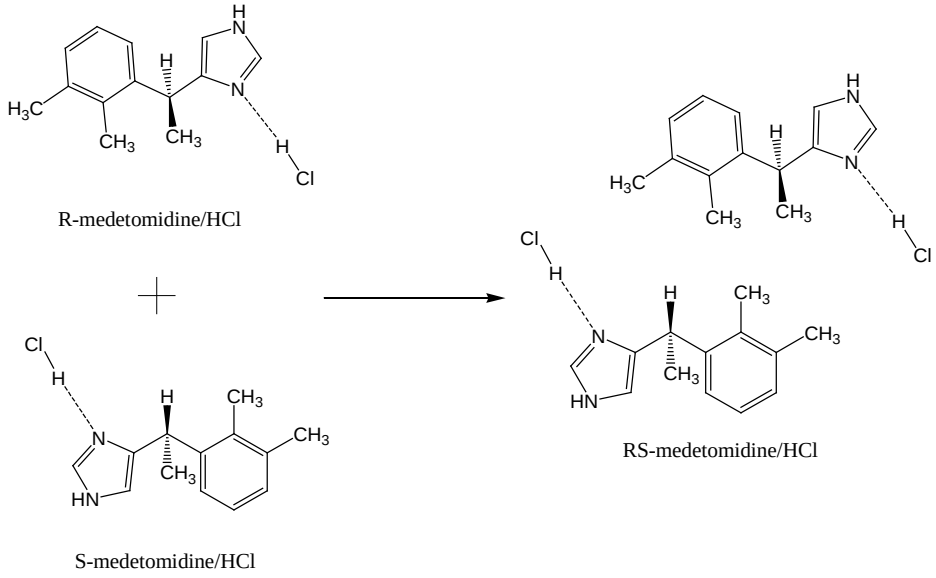

Scheme 1. Sample optimization procedure for the RR, SS and RS structures with acids.

process no symmetry constraints were considered. For example, the R-MM-HCl and S-MM-HCl shown in Scheme 1.

According to the optimized structures in Figure 3, the MM cations and achiral acid anions are positioned as zigzag cylinders. It means that beside each MM cation one acid anion is inserted and the two anions/cations occupy opposite sites and are located in front of each other. In this geometry, ions are partially fixed in their positions through establishing extended network of hydrogen bonding and van der Waals interactions, which are discussed in the AIM section. It should be noted that the observed geometry is exactly similar to what has been previously stated in the experimental work of Kazushi Kinbara et al [1].

After approval of the geometries and the level of theory, the most stable enantiomer was distinguished on the basis of binding, interaction and Gibbs free energy parameters for each complex (Table 2). The obtained binding energy values of R, S, and RS-MM-HCl

Table 2. Comparison of the stability energy values of complexes, in kcal/mol. The energies of the (RR) and (SS) complexes are equal.

Complexes	E_{bind}	ΔG	$E(def)_{MM}$	$E(def)_{acid}$	E_{int}	BSSE	$E_{int+BSSE}$
(RR)-MM-AC	-28.5	1.8	551.5	331.5	-911.5	12.6	-898.9
(RS)-MM-AC	-37.8	-4.4	552.3	330.4	-920.5	12.4	-908.1
(RR)-MM-OX	-55.6	-21.5	552.7	331.8	-940.1	15.4	-924.7
(RS)-MM-OX	-39.8	-1.8	558.6	334.8	-933.2	15.3	-917.9
(RR)-MM-HCl	-38.6	-17.9	552.5	329.6	-920.7	11.4	-909.3
(RS)-MM-HCl	-45.3	-20.8	551.2	326.3	-922.8	10.8	-912.0
(RR)-MM-B	-36.7	-17.5	555.6	321.7	-914.0	12.4	-901.6
(RS)-MM-B	-41.8	-19.9	554.3	320.3	-916.4	12.8	-903.6
(RR)-MM-P	-23.7	8.4	559.6	338.4	-921.7	12.5	-909.2
(RS)-MM-P	-32.4	7.8	557.7	330.2	-920.3	13.3	-907.0

structures shows that energies of RR and SS enantiomers are the same. However, the energy of the RS conglomerate is quite different from the SS and RR complexes.

According to Table 2, RS enantiomer has less energy and more stability than the RR enantiomer except the case of (RR)-MM-Oxalic acid. Furthermore, according the Gibbs free energy values, formation of (RR)-MM-AC, (RR)-MM-P and (RS)-MM-P is not spontaneous and it is not recommended to use propanoic acid for MM crystallization whereas employing oxalic acid is suggested. As the last but not the least point, the deformation energies of all the acids and MM is approximately similar in all the conglomerates while acetic acid provides the lowest MM deformation energy and benzoic acid is associated with the lowest acid deformation energy.

AIM and NBO analysis

Nature of the H. . . X (X=N, Cl or O) hydrogen bonding (HB) were investigated by employing QTAIM theory [21] and all the relevant descriptors were calculated at BCPs and RCPs that are listed in Table 3. The critical points and bond paths of hydrogen bonding are shown in Figure 4. According to Figure 4, when the (R) and (S) MM enantiomers and the acids are put together, they interact and several BCPs and even RCPs can be detected. The RCPs are formed in the middle of six member's cycles and involve HB.

As shown in Table 3, the electron density values of ρ(r) in the BCP of HBs are lower than the electron density values corresponding to covalence bonds. In this regard, the ρ(r) values of the N…H and O…H bonds are in the range of 0.012-0.370 a.u. meantime the O…H values are higher than N…H bond values, in most cases. Decreasing of the ρ(r) values in the O–H covalence bond is further than N–H bond. This point is in agreement with elongation of their bonds (O–H>N–H). To sum up, high ρ(r), more elongation of the O–H bond, low N…H distance and linearity of the N…$H^{+}O^{-}$ angle

Table 3. Introduced indicatives of covalence and hydrogen bonding for complexes that are obtained from the QTAIM theory.

Complexes	Bonds	ρ(r)	$\nabla^2\rho(r)$	H(r)	|V(r)|/G(r)
(RR)-MM-AC	N_{58}-H_{60}	0.3181	-2.0524	-0.6043	18.8701
	H_{60} O_{72}	0.0371	0.1498	-0.0762	1.0117
	O_{73}...H_{32}	0.3704	0.1496	-0.0761	1.0113
	O_{34}...H_{71}	0.0370	0.1497	-0.0762	1.0117
	N_{19}-H_{21}	0.3181	-2.0526	-0.6043	18.8737
(RR)-MM-OX	N_{19}-H_{21}	0.3191	-2.0734	-0.6122	18.5664
	$H_{21}^{+}O_{33}^{-}$	0.03795	0.1342	-0.0726	1.0514
	O_{34}...H_{53}	0.0156	0.0783	-0.02810	0.7679
	O_{38}...H_{71}	0.0154	0.0770	-0.0275	0.7650
	O_{73}...H_{14}	0.0155	0.0709	-0.0283	0.8459
	N_{58}-H_{60}	0.3161	-2.0462	-0.6055	18.3413
(RS)-MM-OX	N_{58}-H_{60}	0.3159	-2.0237	-0.6007	18.0155
	$H_{60}^{+}O_{72}^{-}$	0.0400	0.1413	-0.0775	1.0615
	O_{73}...H_{14}	0.0136	0.0573	-0.0223	0.8281
	O_{77}...H_{20}	0.0154	0.0769	-0.0275	0.7653
	O_{35}...H_{53}	0.0122	0.0573	-0.0215	0.8019
	N_{18}-H_{32}	0.3034	-1.9631	-0.5862	17.4277

Table 3. Ctd

(RS)-MM-Cl	N_{19}-H_{32}	0.3250	-2.1027	-0.6183	19.0106
	$H_{32}^{+}Cl_{66}^{-}$	0.0243	0.0781	-0.0369	0.09614
	Cl_{66}...H_{65}	0.0240	0.0770	-0.0364	0.9613
	N_{53}-H_{64}	0.3261	-2.0914	-0.6181	18.4615
(RS)-MM-P	N_{56}-H_{76}	0.3038	-1.9539	-0.5882	16.6944
	$H_{76}^{+}O_{75}^{-}$	0.0510	0.1627	-0.1015	1.1418
	O_{74}...H_{14}	0.0224	0.1020	-0.0421	0.8697
	O_{36}...H_{58}	0.0268	0.1253	-0.0537	0.8958
	N_{19}-H_{38}	0.2873	-1.809	-0.5527	15.5228

leads to transfer of hydrogen atom (H(60), H(21), H(60), H(32), H(76)) to nitrogen of medotomedine ring and formation of covalent bond, respectively (this process and numbering of hydrogen is displayed in Figure 3 with red circles and Table 3). In addition, AIM calculations confirm ionic bonding between the transferred hydrogen and the oxygen atom of acids. Small values of the $\nabla^2\rho(r)$ and the H(r) in hydrogen bonding of H...O indicate that the nature of these bonds are electrostatic.

Positive and negative values of the $\nabla^2\rho(r)$ in the O–H and N–H bonds implies that these bonds have ionic and covalence natures. Low negative values of the H(r) descriptor in the O–H bonds signify that the covalence nature of such bonds has been decreased.

Although QTAIM is useful to investigate HB, ionic

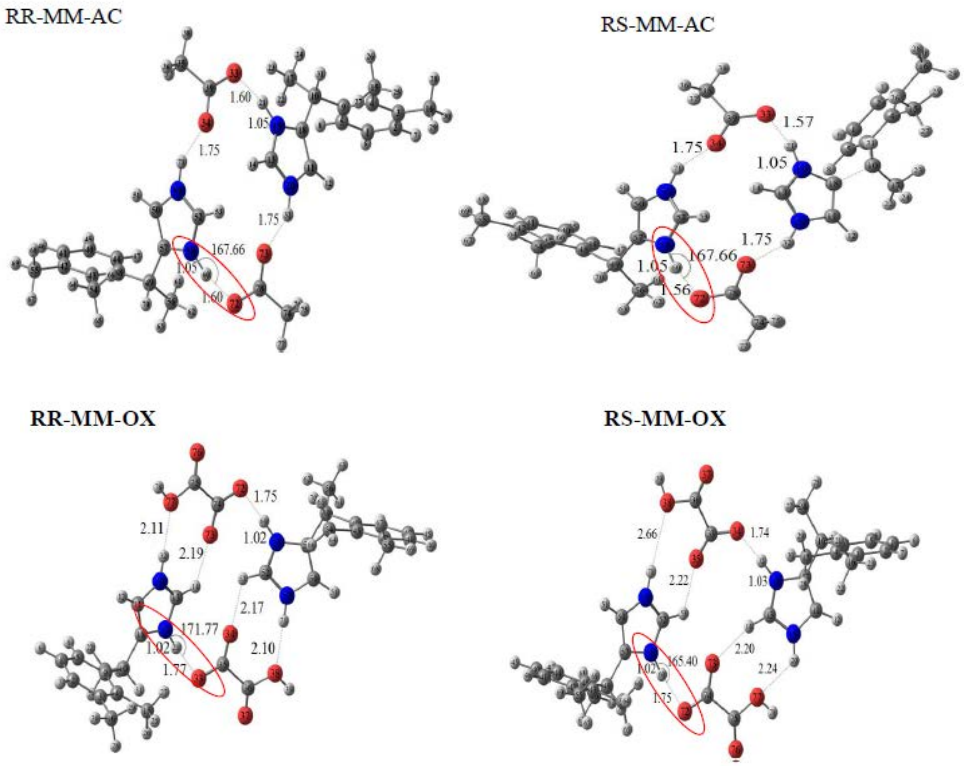

Figure 3. Optimized structure of the complexes, in the R-MM-acids enantiomer. The bond lengths refer to H. . . X (X=N, Cl, O) bond distances.

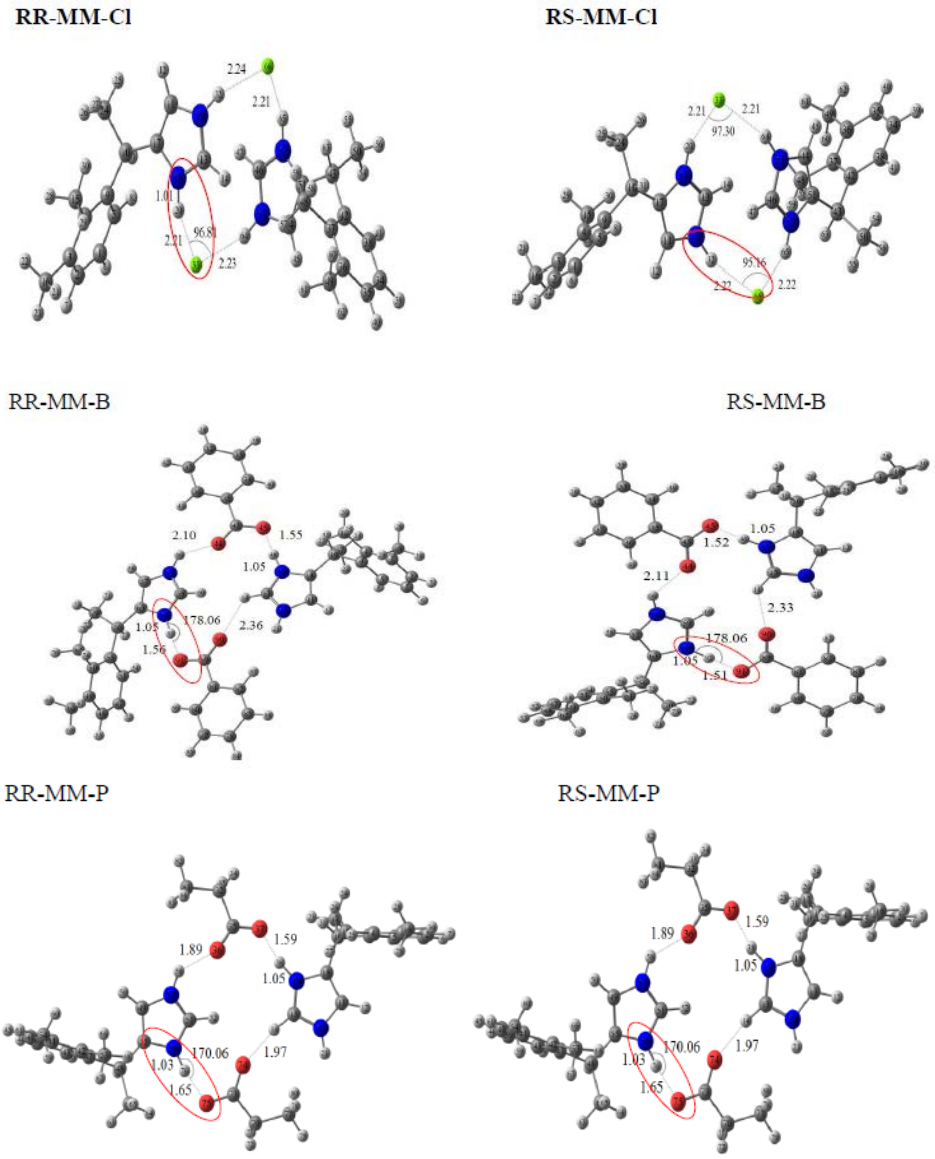

Figure 3. Ctd

and covalent bonds, this method cannot identify source of changes [21]. As a consequence, natural bond orbital (NBO) analysis of HB introduced by Weinhold and co-workers [22] was applied and the most noticeable results are reported in Table 4.

NBO results demonstrate that (RS)-MM-HCl complex has four significant donor-acceptor interactions: $n_{Cl(66)} \rightarrow \sigma^*_{N(19)–H(32)}$, $n_{Cl(66)} \rightarrow \sigma^*_{N(52)–H(65)}$, $n_{Cl(33)} \rightarrow \sigma^*_{N(18)–H(20)}$ and $n_{Cl(33)} \rightarrow \sigma^*_{N(53)–H(64)}$ with stabilization energies of 12.65, 4.96, 15.44, and 14.02 kcal/mol, respectively. There are two types of significant donor-acceptor interactions in other complexes which consists of $n_{N\,(O)} \rightarrow \sigma^*_{N\,(O)–H}$ and $\sigma_{C\,(N,\,O)–H\,(O,\,N)} \rightarrow \sigma^*_{C\,(N,\,O)–H\,(O,\,N)}$. According to Table 4, $n_{N\,(O)} \rightarrow \sigma^*_{N\,(O)–H}$ interaction is stronger than $\sigma_{C\,(N,\,O)–H\,(O,\,N)} \rightarrow \sigma^*_{C\,(N,\,O)–H\,(O,\,N)}$ that is in agreement with AIM analysis. Change of charge values in the H atom which is bridged in N–H is mainly higher than O…H hydrogen bonding. This point confirms strong donor-acceptor interaction in the N–H bond.

Finally, the most considerable charge transfer refers to RS-MM-P while the lowest charge transfer is related

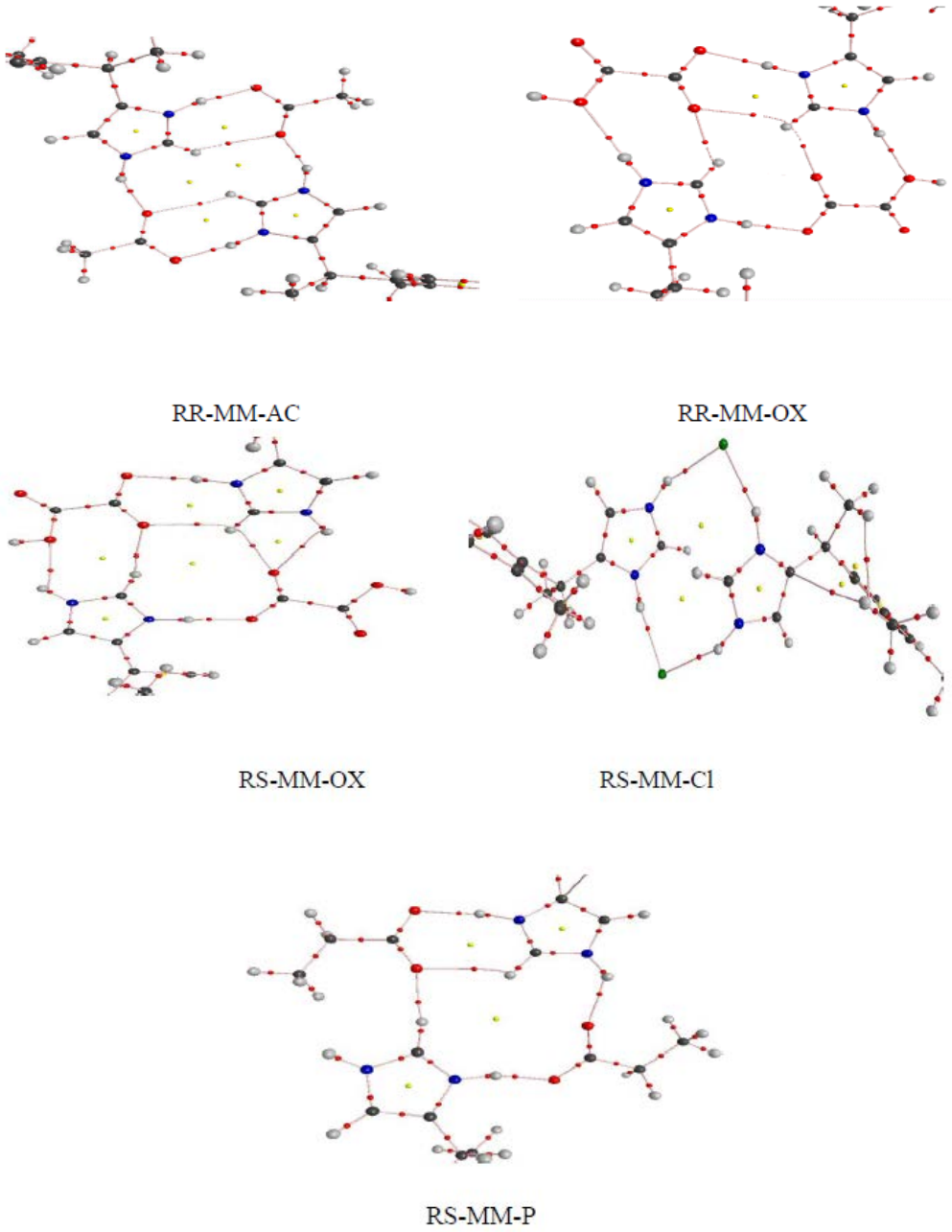

Figure 4. Molecular graphs of the complexes including bond (red color) and ring (yellow color) critical points.

to RS-MM-OX. Therefore, the conglomerates with the highest and lowest charge transfer energies have illustrated the lowest and highest favorability of crystallization, when their Gibbs free energies are re-addressed.

Conclusion

In this study, several conglomerate structures of (R) and (S) medetomidine enantiomers with different achiral acids were optimized and the interaction between the acids and the enantiomers were investigated. According to the results, (RR) and (SS) conglomerates with Oxalic acid are more stable than the (RS) racemic mixture.

Therefore, it can be concluded that for obtaining racemic mixtures (RS), one can use acetic acid solvent while for obtaining identical mixture of (RR) (conglomerate), one can use Oxalic acid solvent. Also, employing Propanoic acid for MM crystallization is not recommended due to the non-spontaneous nature of the

Table 4. Significant donor-acceptor interactions and their corresponding charge transfer energies, in all complexes.

Complex	$\Omega_i \rightarrow \Omega^*_j$	ΔE_{CT}
(RR)-MM-AC	$n_{O(33)} \rightarrow \sigma^*_{N(19)-H(21)}$	44.6
	$n_{O(34)} \rightarrow \sigma^*_{N(59)-H(71)}$	10.4
	$n_{O(73)} \rightarrow \sigma^*_{N(20)-H(32)}$	10.4
	$n_{O(72)} \rightarrow \sigma^*_{N(58)-H(60)}$	44.4
(RR)-MM-OX	$n_{O(33)} \rightarrow \sigma^*_{N(19)-H(21)}$	5.5
	$n_{O(38)} \rightarrow \sigma^*_{N(20)-H(32)}$	5.2
	$\sigma^*_{O(77)-H(78)} \rightarrow \sigma^*_{N(20)-H(32)}$	8.4
	$n_{O(72)} \rightarrow \sigma^*_{N(58)-H(21)}$	31.4
(RS)-MM-B	$n_{O(90)} \rightarrow \sigma^*_{N(20)-H(21)}$	57.4
	$n_{O(91)} \rightarrow \sigma^*_{N(19)-H(46)}$	61.2
	$n_{O(91)} \rightarrow \sigma^*_{N(65)-H(66)}$	11.5
(RS)-MM-OX	$\sigma^*_{C(13)-N(19)} \rightarrow \sigma^*_{O(77)-H(78)}$	9.95
	$\sigma^*_{N(58)-H(60)} \rightarrow \sigma^*_{C(13)-N(19)}$	4.46
	$\sigma^*_{C(52)-N(58)} \rightarrow \sigma^*_{O(77)-H(78)}$	5.62
	$\sigma^*_{O(77)-H(78)} \rightarrow \sigma^*_{C(13)-N(19)}$	9.54
(RS)-MM-P	$n_{O(37)} \rightarrow \sigma^*_{N(19)-H(38)}$	48.01
	$n_{O(36)} \rightarrow \sigma^*_{N(56)-H(76)}$	8.76
	$\sigma^*_{C(35)-O(36)} \rightarrow \sigma^*_{N(56)-H(76)}$	8.16
(RS)-MM-HCl	$n_{Cl(66)} \rightarrow \sigma^*_{N(19)-H(32)}$	12.65
	$n_{Cl(66)} \rightarrow \sigma^*_{N(52)-H(65)}$	4.96
	$n_{Cl(33)} \rightarrow \sigma^*_{N(18)-H(20)}$	15.44
	$n_{Cl(33)} \rightarrow \sigma^*_{N(53)-H(64)}$	14.02

crystallization procedure.

Acknowledgement

The authors gratefully thank from Physical Chemistry research group especially Dr. Fazlolah Eshghi due to highly his suggestions and helping in this study.

References

1. Somagoni J., Eaga Ch., Sunil R., Sarangapani M. Chiral interaction and chiral inversions – new challenges to chiral scientists., IJCP (2019).
2. Kozma D., Böcskei Z., Simon K., Fogassy E. Racemic compound formation–conglomerate formation. Part. 1. Structural and thermoanalytical study of hydrogen phthalate and hydrogen succinate of α-phenylethylamine, *J. Chem. Soc., Perkin Trans.* **2**: 1883-1886 (1994).
3. Shtykova L., Ostrovskii D., Jacobsson P., Nydén M. Interaction between medetomidine and alkyd resins: NMR and FTIR investigation of antifouling marine paint model systems, *J. appl. polym. sci*. **99**: 2797-2809 (2006).
4. Nguyen L. A., He H., Pham-Huy C. Chiral drugs: an

overview, *Int. J. Biomed. Sci*. **2**: 85-100 (2006).
5. Sekhon B. S. Exploiting the power of stereochemistry in drugs: an overview of racemic and enantiopure drugs, *J. Mod. Med. Chem*. **1**: 10-36 (2013).
6. Lin G.-Q., You Q.-D., Cheng J.-F. Chiral drugs: Chemistry and biological action, *John Wiley & Sons*. (2011).
7. Bruno G., Lucia B., Leo Z., Rosella F., Roberto C. Direct separation of the enantiomers of oxaliplatin on a cellulose-based chiral stationary phase in hydrophilic interaction liquid chromatography mode, J. Chromatography A. 1339: 210-213 (2014).
8. Choobdari E., Fakhraian H., Peyrovi M. H. Anion effect on the binary and ternary phase diagrams of chiral medetomidine salts and conglomerate crystal formation, *Chirality*. **26**: 183-188 (2014).
9. Jochen B, Francesco S., Matthew F., The added value of small-molecule chirality in technological applications., Nature Reviews Chemistry. 1: (2017).
10. Vavra J., Severa L. S., Cisarova I., Klepetarova B., Saman D., Koval D., Kasicka V., Teply F., Search for Conglomerate in Set of [7] Helquat Salts: Multigram Resolution of Helicene–Viologen Hybrid by Preferential Crystallization, *J. org. chem*. **78**: 1329-1342 (2012).
11. Leyla C., René S., Hugo M., Elias V., Floris P. Viedma ripening: a reliable crystallisation method to reach single chirality., *Chem. Soc. Rev.* 44: 6723-6732 (2015).
12. Kuusela E., Raekallio M., Anttila M., Falck I., Molsa S., Vainio O. Clinical effects and pharmacokinetics of medetomidine and its enantiomers in dogs, *J Vet Pharmacol Ther*. **23**: 15-20 (2000).
13. Murrell J. C., Hellebrekers L. J. Medetomidine and dexmedetomidine: a review of cardiovascular effects and antinociceptive properties in the dog, *Vet Anaesth Analg*.. **32**: 117-127 (2005).
14. Cullen L. Medetomidine sedation in dogs and cats: a review of its pharmacology, antagonism and dose, *Brit. Vet. J*. **152**: 519-535 (1996).
15. Choobdari E., Fakhraian H., Peyrovi M. H. Prediction and experimental determination of the binary and ternary phase diagrams of (±) medetomidine hydrochloride, *Tetrahedron: Asym.* **24**: 801-806 (2013).
16. Karjalainenc A. Crystal Structure, Thermal Behaviour, Protonation and Mass Spectroscopic Studies of Racemic 4-[1-(2, 3-Dimethylphenyl)-ethyI]-1H-imidazole Hydrochlorides, *Acta. Chem. Scand.* **42**: 537-545 (1988).
17 Frisch M., Trucks G., Schlegel H., Scuseria G., Robb M., Cheeseman J., Scalmani G., Barone V., Mennucci B., Petersson G., Gaussian 09W, Revision A. 1. Wallingford (CT): Gaussian, Inc, (2009).
18. McLean A., Chandler G. Contracted Gaussian basis sets for molecular calculations. I. Second row atoms, Z= 11–18, *J. Chem. Phys*. **72**: 5639-5648 (1980).
19. Tirado-Rives J., Jorgensen W.L. Performance of B3LYP density functional methods for a large set of organic molecules, *J. Chem. Theor. & Comput*. **4**: 297-306 (2008).
20. Pakiari A.H., Eshghi F., Geometric and Electronic Structures of Vanadium Sub-nano Clusters, Vn (n = 2-5), and their Adsorption Complexes with CO and O2 Ligands: A DFT-NBO Study. *Phys. Chem. Res.* **5**: 601-615 (2017).
21. Bader R., Nguyen-Dang T., Tal Y. A topological theory of molecular structure, *Rep. Prog. Phys.* **44**: 893 (1981).
22. Foster J., Weinhold F. Natural hybrid orbitals, *J. Am. Chem. So*c. **102**: 7211-7218 (1980).
23. Reed A. E., Weinstock R. B., Weinhold F. Natural population analysis, *J. Chem. Phys*. **83**: 735-746 (1985).
24. Exprimental data taked such as bond lenght from this website "www.http://cccbdb.nist.gov/".